Improved time-resolved acousto-optic technique for optical fiber analysis of axial non-uniformities by using edge interrogation

E. P. Alcusa-Sáez,[1] A. Díez,[1,*] M. González-Herráez,[2] and M. V. Andrés[1]

[1]*Departamento de Física Aplicada y Electromagnetismo-ICMUV, Universidad de Valencia, Dr. Moliner 50, 46100 Burjassot, Spain*

[2]*Departamento de Electrónica, Universidad de Alcalá, Escuela Politécnica DO 231, 28871Alcalá de Henares, Spain*

[*]*antonio.diez@uv.es*

Abstract: The time-resolved acousto-optic technique demonstrated recently to be a very useful method for the analysis of fiber axial non-uniformities, able to detect variations of fiber diameter in the nanometric scale with a spatial resolution of few cm. An edge interrogation approach is proposed to improve further the performance of this technique. The detection of subnanometer fiber diameter changes or sub-ppm changes of the core refractive index is demonstrated.

OCIS codes: (060.2270) Fiber characterization; (230.1040) Acousto-optical devices.

References and links

1. J. F. Brennan, "Dispersion management with long-length fiber Bragg gratings," in *Optical Fiber Communication Conference*, Technical Digest (Optical Society of America, 2003), paper FC1.
2. D. K. Serkland and P. Kumar, "Tunable fiber-optic parametric oscillator," Opt. Lett. **24**(2), 92–94 (1999).
3. J. E. Sharping, M. Fiorentino, P. Kumar, and R. S. Windeler, "Optical parametric oscillator based on four-wave mixing in microstructure fiber," Opt. Lett. **27**(19), 1675–1677 (2002).
4. J. Rarity, J. Fulconis, J. Duligall, W. J. Wadsworth, and P. St. J. Russell, "Photonic crystal fiber source of correlated photon pairs," Opt. Express **13**(2), 534–544 (2005).
5. P. Di Vita and U. Rossi, "Backscattering measurements in optical fibres: separation of power decay from imperfection contribution," Electron. Lett. **15**(15), 467–469 (1979).
6. K. Nakajima, M. Ohashi, and M. Tateda, "Chromatic dispersion distribution measurement along a single-mode optical fiber," J. Lightwave Technol. **15**(7), 1095–1101 (1997).
7. M. Sumetsky and Y. Dulashko, "Radius variation of optical fibers with angstrom accuracy," Opt. Lett. **35**(23), 4006–4008 (2010).
8. E. P. Alcusa-Sáez, A. Díez, M. González-Herráez, and M. V. Andrés, "Time-resolved acousto-optic interaction in single-mode optical fibers: Characterization of axial nonuniformities at the nanometer scale," Opt. Lett. **39**(6), 1437–1440 (2014).
9. H. S. Kim, S. H. Yun, I. K. Kwang, and B. Y. Kim, "All-fiber acousto-optic tunable notch filter with electronically controllable spectral profile," Opt. Lett. **22**(19), 1476–1478 (1997).
10. S. D. Lim, K. J. Park, S. Eom, J. M. Jeong, B. Y. Kim, and S. B. Lee, "Ultrawidely tunable single-mode fiber acousto-optic filter," Opt. Lett. **36**(7), 1101–1103 (2011).

1. Introduction

At present, optical fiber fabrication techniques meet extraordinary uniformity requirements. With respect to diameter control, a standard deviation of 0.2 μm in fibers with 125 μm diameter is readily achieved. In the same way, compositional control allows constancy of refractive index for kilometer fiber lengths. In practice, such a level of uniformity is sufficient for most applications. However, in some specific utilizations of fiber optics, even smaller non-uniformities along the fiber can have an impact on their performance. Particularly, in applications where a phase-matching condition must be satisfied along a given fiber length, as for example, in the fabrication of long fiber Bragg gratings [1], long-period gratings, or applications based on the generation of parametric nonlinear processes in optical fibers [2–4].

Accurate characterization of the local variations of the optical fiber properties may be important for the improvement of these types of applications, and also can eventually provide useful information for the improvement of the fiber drawing process. Techniques to measure

#231641 - $15.00 USD Received 30 Dec 2014; revised 11 Feb 2015; accepted 16 Feb 2015; published 11 Mar 2015

fluctuations of dispersion and mode field diameter along an optical fiber have been developed in the last two decades [5,6], although usually with spatial resolutions much longer than 1 meter. The detection of local variations of the fiber radius in the angstrom scale along sections of fiber few cm long, was demonstrated using a technique based on the excitation of whispering-gallery mode resonances [7].

Recently, we reported on the use of a time-resolved acousto-optic (AO) technique for the analysis and characterization of axial non-uniformities in singlemode optical fibers [8]. It is based on the propagation of a short packet of a flexural wave along the fiber, which causes coupling between the core and a cladding mode. The elastic packet propagates along the fiber at its group velocity, thus, at a given instant the optical transmittance is determined by the coupling at the specific fiber point where the elastic packet is located. Fluctuations of the fiber properties along the section under analysis produce fluctuations of the AO phase-matching wavelength, which in turn causes fluctuations of the optical transmittance at a given wavelength. In [8], detection of fiber diameter variations in the nanometric scale was demonstrated by monitoring the fluctuations in the optical transmittance at the optical wavelength matching the AO resonance. In this paper, we show that some limitations of the technique can be overcome, and the sensitivity can be improved significantly, by monitoring the transmittance fluctuations at a specific out-of-resonance optical wavelength.

2. Fundamentals

A flexural elastic wave propagating along an optical fiber creates a periodic refractive-index perturbation that can cause coupling between the core mode and co-propagating cladding modes [9,10]. In a single-mode fiber, coupling between the core and a cladding mode produces a notch in the spectrum of the light transmitted. The light intensity propagating in the core mode, can be calculated using coupling mode theory,

$$T = 1 - \frac{\kappa^2}{\kappa^2 + \delta^2} \mathrm{Sin}^2 [\, L_{eff} \sqrt{\kappa^2 + \delta^2}\,] \tag{1}$$

where L_{eff} is the AO interaction length, κ is the coupling coefficient related to the strength of the index perturbation and to the overlap of the index perturbation and the optical fields. The parameter δ is the so-called detuning parameter and is given by,

$$\delta = \pi \cdot \left(\frac{\Delta n_m}{\lambda} - \frac{1}{\Lambda} \right) \tag{2}$$

where Δn_m is the difference between the modal indices of the core and the cladding mode, λ is the optical wavelength, and Λ is the wavelength of the elastic wave. The transmittance is minimum when the phase-matching condition is satisfied ($\delta = 0$) and optimum coupling is achieved. The resonance wavelength, λ_R, at which this condition happens is $\lambda_R = \Delta n_m \cdot \Lambda$.

For an elastic perturbation of a given frequency Ω, the resonance wavelength is determined by the fiber properties. Fluctuations of the fiber properties lead to the shift of the notch, and consequently, to variations of the optical transmittance at a given optical wavelength. Given the transmittance for a specific value of detuning δ_0, the transmittance at a detuning δ in the vicinity of δ_0, can be approximated by a Taylor series expansion,

$$T(\delta) \approx T(\delta_0) + \left(\frac{\partial T}{\partial \delta} \right)_{\delta_0} (\delta - \delta_0) + \frac{1}{2} \left(\frac{\partial^2 T}{\partial \delta^2} \right)_{\delta_0} (\delta - \delta_0)^2 + \ldots \tag{3}$$

Figure 1 shows, as a function of δ, the transmittance, the first, and the second derivatives of transmittance with respect to δ. At $\delta = 0$, the first derivative is zero while the second derivative reaches its maximum value. Therefore, near $\delta = 0$, the transmittance is given to a second-order approximation by,

#231641 - $15.00 USD Received 30 Dec 2014; revised 11 Feb 2015; accepted 16 Feb 2015; published 11 Mar 2015

$$T(\delta) \approx T(\delta = 0) + \frac{1}{2}\left(\frac{\partial^2 T}{\partial \delta^2}\right)_{\delta=0} \delta^2 \tag{4}$$

Equation (4) indicates that the modulus of the detuning can be obtained from the difference between the optical transmittance and the transmittance at resonance, provided that the rest of parameters (L_{eff} and κ) are known. The experimental results reported in [8] were based on these conditions: the optical wavelength was tuned to achieve minimum transmittance and the fluctuation of the detuning along the fiber was obtained from Eq. (4). This manner of addressing the issue presents two limitations. First, the sign of the detuning cannot be determined, and second, the sensitivity of the method is far from its optimum since the change of transmittance with detuning is very small around $\delta = 0$.

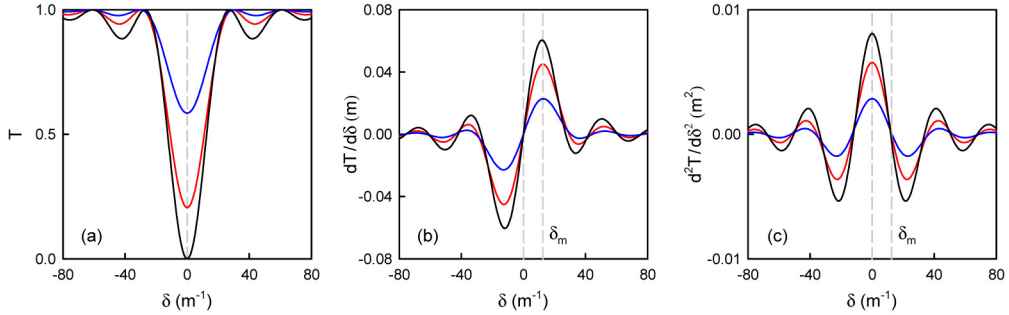

Fig. 1. (a) Transmittance, (b) first, and (c) second derivative of transmittance with respect to detuning, as a function of detuning. L_{eff} = 10 cm, κ = 15.7 m^{-1} (black), κ = 11 m^{-1} (red), κ = 7 m^{-1} (blue). Vertical lines indicates $\delta = 0$ and δ_m.

The two limitations can be overcome by looking at the fluctuations of transmittance around the value of $\delta = \delta_m$, where δ_m is the detuning at which $\partial T/\partial \delta$ is maximum (see Fig. 1(b)). At δ_m, the second derivative, $\partial^2 T/\partial \delta^2$, is zero, thus, the transmittance near δ_m can be approximated by,

$$T(\delta) \approx T(\delta_m) + \left(\frac{\partial T}{\partial \delta}\right)_{\delta_m} (\delta - \delta_m) \tag{5}$$

From Eq. (5), the fluctuation of the detuning can be obtained from the variation of the optical transmittance with respect to the transmittance at δ_m. In Fig. 2(a), we compare the change of transmittance caused by a small change of detuning around $\delta_0 = 0$ and $\delta_0 = \delta_m$. It is clear that a small change of detuning leads to a larger change in transmittance in the second case. This happens no matter the value of $\kappa \cdot L_{eff}$. It is also pointed out that the sensitivity increases as $\kappa \cdot L_{eff}$ approaches $\pi/2$. Notice that at $-\delta_m$, $\partial T/\partial \delta$ has the same modulus but opposite sign. Thus, a given change of the fiber properties leads to a change of transmittance with the same magnitude as when $\delta = \delta_m$ but with opposite sign.

In Fig. 2(b), we analyze the error that involves the linear approximation of the transmittance stated in Eq. (5). The relative error is shown for two representative values of $\kappa \cdot L_{eff}$. Of course, the deviation from linearity increases as δ differs from δ_m. The effect becomes more pronounced as the strength of the notch increases. The most unfavorable case is when $\kappa \cdot L_{eff} = \pi/2$. Nonetheless, it is worth to note that there is a wide range of variation of δ for which the relative error is within ± 1%.

The use of Eq. (5) requires the measurement of the transmittance at δ_m instead of at resonance. From the experimental point of view, it does not add any difficulty, since it can be achieved, for example, by simply shifting the optical wavelength in an appropriate amount, which is straight forward if a tunable laser source is used.

#231641 - $15.00 USD Received 30 Dec 2014; revised 11 Feb 2015; accepted 16 Feb 2015; published 11 Mar 2015

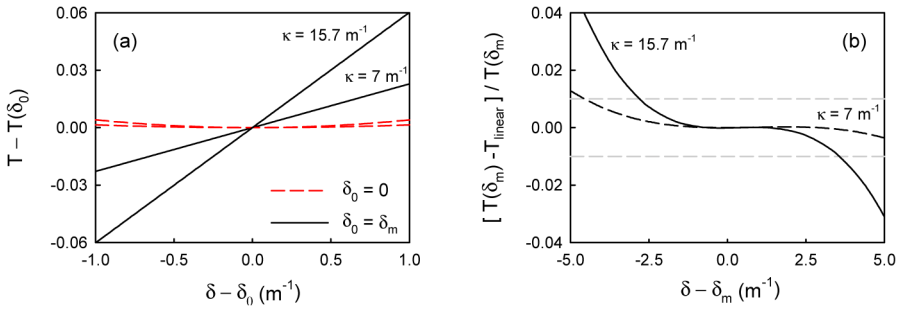

Fig. 2. (a) Change of transmittance with respect to transmittance at $\delta_0 = 0$ (red line) and at $\delta_0 = \delta_m$ (black line) caused by a small change of detuning. (b) Relative error that results when the transmittance at a given δ near δ_m is approximated by Eq. (5).

3. Experimental results and discussion

The experimental setup used for the experiments was described in detail in [9]. Elastic wave packets were generated by a piezoelectric disk and coupled to the fiber via a horn. The flexural elastic packets propagated along a section of unjacketed fiber and were absorbed by an acoustic damper at the end of the interaction region. The piezoelectric was driven with an electrical signal consisting of a burst of 20 periods of a sinusoidal RF signal of frequency Ω. The duration of the resulting elastic wave packet was 30 μs. The optical signal was provided by a tunable, linearly polarized laser emitting in the C band. A polarization controller was used to adjust the polarization state of the input light. The optical transmission was measured as a function of time as an elastic packet propagated along the fiber.

Figure 3(a) shows the transmittance recorded as the elastic wave packet propagated along a particularly uniform section of SMF-28 fiber of 1.45 m in length. The frequency of the burst signal was 2.1 MHz. The attenuation shown in the transmittance traces results from the coupling between the LP_{01} and the LP_{11} cladding mode. The three traces are for the three different optical wavelengths at which the detuning was $\delta_0 = 0$ (black line), $\delta_0 \gg \delta_m$ (red line) and $\delta_0 \gg -\delta_m$ (blue line), respectively.

Several features common to all traces can be pointed out. The two transients at $t = 0$ and $t = 0.5$ ms are related with the time that the elastic packet takes to enter and to leave the interaction region, respectively. From the transient time, we can obtain the effective length of the elastic perturbation on the fiber, $L_{eff} = 8.3$ cm (the group velocity was obtained from the time that the elastic packet requires to propagate along the whole fiber length resulting $v_g = 2800$ m/s). The recovery of the transmittance as the elastic packet propagates along the fiber is caused by the attenuation of the elastic wave. The coupling coefficient κ is proportional to the elastic amplitude, thus, the attenuation of the elastic wave leads to the reduction of the coupling strength. The coupling coefficient varies along the fiber as follows,

$$\kappa = \kappa_0 \cdot e^{-\alpha \cdot z} \tag{6}$$

where $z = v_g \cdot t$ is the propagation distance, κ_0 is the coupling coefficient at $z = 0$, and α is the attenuation coefficient of the elastic wave.

In addition to the exponential recovery, one can observe small fluctuations of the transmittance as the elastic packet propagates along the fiber. These fluctuations are caused by small shifts of the AO resonant coupling wavelength due to fluctuations of the fiber properties along its length [8]. It is worth to note that the fluctuations shown by the traces taken at the two edges of the notch are complementary, as expected since the slope at the edges of the notch have opposite sign.

To obtain the fluctuations of detuning along the fiber we analyze first the trace at resonance. Following the procedure described in [8], we obtained $\kappa_0 = 8.16$ m^{-1}, and $\alpha = 0.55$ m^{-1}. The transmittance at resonance in a perfectly uniform fiber as a function of position

#231641 - $15.00 USD Received 30 Dec 2014; revised 11 Feb 2015; accepted 16 Feb 2015; published 11 Mar 2015

calculated using Eqs. (1) and (6) is also shown in Fig. 3(a). Given that the excitation conditions of the elastic wave are identical for all the traces, the values of κ_0 and L_{eff} obtained from the trace at resonance also apply for the traces obtained out of resonance. The experimental value of detuning δ_m for the transmittance recorded at optical wavelengths at the edges of the notch ($\delta = \pm \delta_m$) is obtained by fitting both curves to the transmittance in a perfectly uniform fiber given by Eq. (1), taking into account the elastic attenuation. Figure 3(a) shows the best-fit, obtained with a value of $\delta_m = 15.65\ \mathrm{m}^{-1}$.

The fluctuations of the detuning along the fiber with respect to δ_m can be calculated using Eq. (5). The derivative of the transmittance with respect to the detuning can be related with the derivative of the transmittance with respect to wavelength as follows,

$$\left.\frac{\partial T}{\partial \delta}\right|_{\delta_m} = \left(\frac{\partial \delta}{\partial \lambda}\right)_{\lambda_m}^{-1} \cdot \left.\frac{\partial T}{\partial \lambda}\right|_{\lambda_m} \tag{7}$$

where λ_m is the wavelength at which the detuning is δ_m. The term $\partial T/\partial \lambda \,|_{\lambda_m}$ was obtained experimentally by measuring the transmittance at two wavelengths close to λ_m. Notice that the attenuation of the elastic wave leads to the attenuation of the coupling constant, κ, and this affects the slope at the edge of the transmission notch. In particular, the modulus of $\partial T/\partial \lambda \,|_{\lambda_m}$ decreases with the propagation distance z. Figure 3(b) shows the difference between the transmittance measured experimentally for the optical wavelengths lying at the edges of the notch and the transmittance given by Eq. (1), as a function of fiber position. Finally, the detuning fluctuation along the fiber is obtained from the experimental data, taking into account Eqs. (5) and (7). The result obtained from the transmittance recorded at the optical wavelengths lying at the two edges of the notch is shown in Fig. 3(c). The term $\left(\partial \delta/\partial \lambda\right)_{\lambda_m} = 6.11 \times 10^{-3}\ \mu\mathrm{m}^{-2}$, was calculated numerically assuming a step-index profile fiber with NA = 0.12 and cutoff wavelength = 1.26 μm.

A feasible origin for the detuning fluctuation along the fiber is the non-uniformity of the fiber radius. In that case, one can calculate the fluctuation of radius that would lead to the detuning fluctuation shown in Fig. 3(c). For small radius fluctuations,

$$\left(\delta - \delta_0\right) \approx \left.\frac{\partial \delta}{\partial a}\right|_{a_0} \left(a - a_0\right) \tag{8}$$

where a_0 is the nominal fiber radius. Figure 3(c) also shows the corresponding radius fluctuation. Again, the derivative term of Eq. (8) was calculated numerically, taking into account the nominal parameters of the fiber, the elastic properties of the fiber, and the two modes involved in the coupling.

The sensitivity of the technique depends essentially on the characteristics of the fiber, the acoustic frequency, the optical wavelength, and the modes involved in the AO coupling. For the experiment reported above, assuming that the smallest transmittance deviation able to be detected is 1×10^{-3}, a detuning change of $0.05\ \mathrm{m}^{-1}$ can be resolved. Such detection limit implies that, if the origin of the transmittance deviations is the fluctuation of the fiber radius, a radius variation of 0.4 nm can be detected. If the transmittance deviations would be caused by fluctuations of the core refractive index, then core refractive index variations of 4×10^{-8} could be resolved.

#231641 - $15.00 USD Received 30 Dec 2014; revised 11 Feb 2015; accepted 16 Feb 2015; published 11 Mar 2015

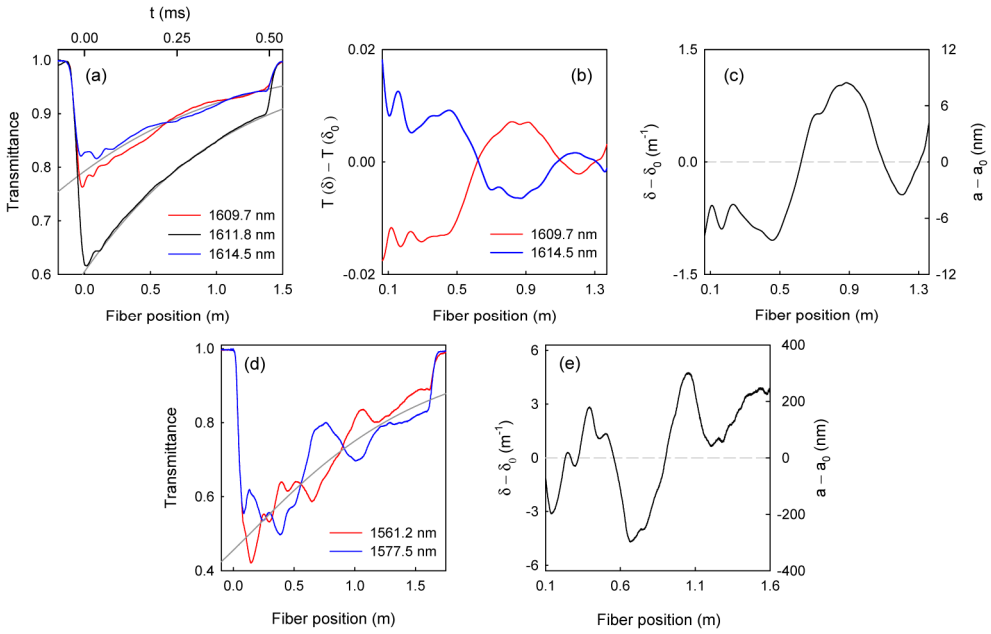

Fig. 3. (a) Transmittance as a function of time/position for different optical wavelengths. Grey lines are the transmittance calculated with Eq. (1) at $\delta = 0$ and at $\delta = 15.65$ m^{-1}. (b) Transmittance fluctuations, and (c) detuning fluctuations along the fiber. (d) Transmittance as a function of fiber position in a segment of Nufern SM-YSF-HI fiber. Grey line is the transmittance calculated with Eq. (1) and $\delta = 15.4$ m^{-1}. (e) Fluctuation of detuning and the corresponding radius fluctuation.

The experiment was repeated with a single-mode, core-pumped YDF (Nufern, SM-YSF-HI, with nominal NA = 0.11, λ_c = 870 nm), and the main results are shown in Figs. 3(d) and 3(e). In this example, the coupled modes were the LP_{01} and LP_{15}, the resonance wavelength 1569 nm and the frequency of the elastic wave 2.1 MHz. Notice that the detuning fluctuation is almost five times larger than in the previous fiber.

It is worth to note that broadening of the elastic packet due to group-velocity dispersion of the flexural mode affects the length resolution of the technique. For our experimental conditions, however, this effect is small. After 1 m, the duration of the elastic packet, and consequently the resolution in length, increases just about 3%. However, it is an issue to be taken into account when shorter packets are used, or longer fiber lengths are analyzed.

4. Conclusion

We have shown that the performance of the time-resolved acousto-optic technique for the analysis of fiber axial non-uniformities can be greatly improved by applying an edge interrogation strategy. Detuning fluctuations as small as 0.05 m^{-1} are detected along sections of 1.5 m long SMF-28 fiber by measuring the transmittance at wavelengths located at the edges of the transmission notch. Such a resolution in detuning enables the detection of subnanometric fiber diameter changes or sub-ppm changes of the core refractive index.

Acknowledgments

Financial support from the Ministerio de Economía y Competitividad of Spain and FEDER funds (project TEC2013-46643-C2-1-R), and the Generalitat Valenciana (project PROMETEOII/2014/072) is acknowledged. MGH acknowledges support from the European Research Council through Starting Grant U-FINE (Grant no. 307441).

#231641 - $15.00 USD Received 30 Dec 2014; revised 11 Feb 2015; accepted 16 Feb 2015; published 11 Mar 2015